

1 **Identification of the maize Mediator CDK8 module, and**
2 ***Dissociation* insertional mutagenesis of *ZmMed12a***

3

4 **Tania Núñez-Ríos^{1†}, Kevin R. Ahern², Ana Laura Alonso-Nieves¹, Daniel Lepe-Soltero¹,**
5 **Carol Martínez-Camacho^{1†}, Marcelina García-Aguilar¹, Thomas P. Brutnell³, C.**
6 **Stewart Gillmor^{*1} and Ruairidh James Hay Sawers^{*1}**

7 ¹ Laboratorio Nacional de Genómica para la Biodiversidad (LANGEBIO), Unidad de
8 Genómica Avanzada, Centro de Investigaciones y de Estudios Avanzados del Instituto
9 Politécnico Nacional (CINVESTAV-IPN), Irapuato, Guanajuato, México.

10 ² Boyce Thompson Institute for Plant Research, Ithaca, New York, U.S.A.

11 ³ Donald Danforth Plant Science Center, St. Louis, Missouri, U.S.A.

12

13 [†]Current address: PLANAMERICA, Michoacán, México (TN-R); Universidad Intercultural
14 de Chiapas, México (CM-C)

15

16 *Correspondence:

17 Stewart Gillmor & Ruairidh Sawers

18 Laboratorio Nacional de Genómica para la Biodiversidad (LANGEBIO), Unidad de
19 Genómica Avanzada, Centro de Investigaciones y de Estudios Avanzados del Instituto
20 Politécnico Nacional (CINVESTAV-IPN), Irapuato, Guanajuato, México.

21 stewart.gillmor@cinvestav.mx; rusawers@cinvestav.mx

22

23 **ABSTRACT**

24 Mediator is a conserved transcriptional co-activator that links transcription factors bound at
25 enhancer elements to RNA Polymerase II. Mediator-RNA Polymerase II interactions can be
26 sterically hindered by the Cyclin Dependent Kinase 8 (CDK8) module, a submodule of
27 Mediator that acts to repress transcription in response to discrete cellular and environmental
28 cues. The CDK8 module is conserved in all eukaryotes and consists of 4 proteins: CDK8,
29 CYCLIN C (CYCC), MED12, and MED13. In this study, we have characterized the CDK8
30 module of Mediator in maize. The maize genome contains single copy genes for *Cdk8*, *CycC*,
31 and *Med13*, and two genes for *Med12*. Analysis of expression data for the CDK8 module
32 demonstrated that all five genes are broadly expressed in maize tissues, with *ZmMed12a*,
33 *ZmMed12b*, and *ZmMed13* exhibiting similar expression patterns. We performed a
34 *Dissociation (Ds)* insertional mutagenesis, recovering two independent insertions in the
35 *ZmMed12a* gene. One of these *Ds* insertions results in a truncation of the *ZmMed12a*
36 transcript. Our molecular characterization of the maize CDK8 module, as well as transposon
37 tagging of *ZmMed12a*, establish the basis for molecular and functional studies of these
38 important transcriptional regulators in *Zea mays*.

39

40 **KEYWORDS** *Zea mays*, Dissociation, Mediator, CDK8 module, Med12, Med13, CycC

41

42 INTRODUCTION

43 Transcriptional regulation plays an essential role in almost all aspects of development and
44 physiology, including responses to the biotic and abiotic environment. One key regulator of
45 transcription is Mediator, a multiprotein complex conserved from yeast to plants to animals,
46 which was initially identified based on its requirement for transcription of virtually all
47 protein-coding genes (Kelleher et al., 1990; Flanagan et al., 1991; Bourbon, 2008). The Core
48 Mediator consists of Head, Middle and Tail domains, and typically functions as a
49 transcriptional co-activator, linking transcription factors bound at upstream enhancer
50 elements to RNA polymerase II (RNA pol II) (reviewed in Yin and Wang, 2014; Allen and
51 Taatjes, 2015). The Head and Middle domains interact with RNA pol II, while the Tail
52 domain is thought to interact with specific transcription factors (Tsai et al., 2014; Robinson et
53 al., 2015; Plaschka et al., 2015; reviewed in Larivière et al., 2012). A fourth Mediator module
54 shows transient association with Core Mediator and often acts to repress transcription. This
55 Cyclin Dependent Kinase 8 (CDK8) module is composed of the proteins MED12, MED13,
56 CYCLIN C (CYCC), and CDK8 (reviewed in Björklund and Gustafsson, 2005). In
57 agreement with the variable association of the CDK8 module with Core Mediator,
58 purification of Mediator from *Arabidopsis thaliana* yielded both conserved Core Mediator
59 subunits, as well as subunits unique to *Arabidopsis*, but did not include components of the
60 CDK8 module (Bäckström et al., 2007).

61 In yeast and animals, components of the CDK8 module can regulate transcription in
62 several ways, with different subunits playing different roles. One mechanism for
63 transcriptional repression involves steric inhibition, where the CDK8 module occupies the
64 Core Mediator pocket that binds RNA pol II, thereby preventing interaction of Core Mediator
65 and RNA pol II (Elmlund et al., 2006; Tsai et al., 2013). Transcriptional repression by this
66 steric mechanism has the potential to be dynamic, as the occupancy of the RNA pol II
67 binding pocket can be modulated during subsequent rounds of assembly of the Mediator-
68 RNA pol II holoenzyme (reviewed in Allen and Taatjes, 2015). This steric mechanism
69 involves all four units of the CDK8 module, with the MED13 subunit playing the most
70 important role, interacting directly with the Middle domain of Core Mediator (Knuesel et al.,
71 2009; Tsai et al., 2013). The MED13 subunit also serves an important function in regulation
72 of CDK8 module stability: phosphorylation of a conserved phosphodegron site in MED13
73 can lead to recognition by a ubiquitin ligase complex, and subsequent degradation (Davis et
74 al., 2013).

75 In *Arabidopsis*, components of the CDK8 module were initially identified by their
76 requirement for development, and also affect the response to fungal pathogens and cellular
77 stress. Mutations in *CDK8* were identified as enhancers of the phenotype of the floral
78 homeotic mutant *hua1hua2*, and thus were named *hua enhancer 3 (hen3)*. *hen3* mutants
79 affect floral organ identity, as well as leaf size and cell shape, and the HEN3 protein was
80 demonstrated to have CDK8 kinase activity (Wang and Chen, 2004). CDK8 regulates

81 retrograde signaling from the mitochondria to the nucleus in response to H₂O₂ and cold stress
82 (Ng et al., 2013). *CDK8*, as well as *MED12* and *MED13*, are also required for the response to
83 both fungal and bacterial pathogens (Zhu et al., 2014).

84 Mutations in *MED12* and *MED13* were initially reported from a genetic screen for
85 regulators of pattern formation in Arabidopsis embryogenesis, and were named *center city*
86 (*cct*) and *grand central* (*gct*), to reflect the increased size of the shoot apical meristem (SAM)
87 in these mutants. *cct* and *gct* mutants delay the timing of pattern formation during
88 embryogenesis, rather than affecting pattern formation *per se*—the increased size of the SAM
89 in *cct* and *gct* mutants can be attributed to its formation later in embryogenesis compared to
90 the wild type (wt) (Gillmor et al., 2010). The delayed formation of the SAM may be related
91 to auxin signaling, as both the *med13* allele *macchi-bou2* (*mab2*), and the *med12* allele
92 *cryptic precocious* (*crp*) act as enhancers of a mutation in the auxin dependent kinase
93 *PINOID* (Furutani et al., 2004; Ito et al., 2011; Imura et al., 2012). Importantly for
94 mechanistic studies of CDK8 module function in Arabidopsis, Ito et al. (2011) demonstrated
95 that the *MED13* and *CDK8* proteins are both able to interact with Cyclin C, as has previously
96 been demonstrated in *Drosophila* (Loncle et al., 2007). Consistent with studies showing
97 auxin-related phenotypes for mutants in *MED12* and *MED13*, a recent study showed that both
98 of these genes, as well as *CDK8*, are involved in auxin transcriptional responses, and that the
99 *MED13* protein relays signals from the *IAA14* protein to repress the auxin responsive
100 transcription factors *ARF7* and *ARF19* (Ito et al., 2016).

101 In addition to affecting the timing of pattern formation in embryogenesis, *MED12* and
102 *MED13* also regulate the timing of post-embryonic phase transitions in Arabidopsis. A
103 dominant allele of *med12* (named *cryptic precocious* (*crp-1D*)) was isolated in a genetic
104 screen for enhancers of the early flowering phenotype conditioned by overexpression of the
105 florigen *FT* (Imura et al., 2012). Loss of function mutants in *crp/cct* and *gct* show late
106 flowering due to overexpression of the floral repressor *FLOWERING LOCUS C* (*FLC*), as
107 well as decreased expression of the floral promoters *FLOWERING LOCUS* (*FT*), *TWIN*
108 *SISTER OF FT* (*TSF*), *SUPPRESSOR OF OVEREXPRESSION OF CONSTANTS 1* (*SOC1*),
109 *APETALA 1* (*API*) and *FRUITFULL* (*FUL*) (Imura et al., 2012; Gillmor et al., 2014). *cct* and
110 *gct* mutants also misexpress seed specific genes during seedling development, and have an
111 elongated vegetative phase due to overexpression of the microRNA miR156 (Gillmor et al.,
112 2014), a master regulator of the vegetative phase in plants (Wu et al., 2009). Taken together,
113 these results demonstrate that *MED12* and *MED13* act as master regulators of developmental
114 timing in plants, regulating the timing of pattern formation in embryogenesis, the seed-to-
115 seedling transition, vegetative phase change, and the transition to flowering (Gillmor et al.,
116 2010; Ito et al., 2011; Imura et al., 2012; Gillmor et al., 2014).

117 Due to its importance in plant development and physiology, we have extended studies of
118 the *CDK8* module to the crop plant maize (*Zea mays*). Establishment of molecular and
119 genetic resources for the study of the maize *CDK8* module will allow evaluation of its role in
120 the regulation of agricultural traits such as timing of flowering and seed development, as well
121 as responses to biotic and abiotic stresses. One of the primary goals of this work was isolation
122 of loss of function mutant alleles of maize *CDK8* module-encoding genes. In maize,
123 resources based on endogenous DNA transposons constitute the most accessible and widely-
124 used technology for reverse genetics (McCarty and Meeley, 2009). The two major transposon

125 systems used for gene tagging in maize are *Activator/Dissociation (Ac/Ds)* and *Mutator (Mu)*
126 (Candela and Hake, 2008). These systems consist of an autonomous or master element that
127 encodes a transposase (TPase) and a second non-autonomous or receptor element. The
128 receptor elements are frequently derived from a master element by mutations within the
129 TPase gene. Lacking TPase, non-autonomous elements are stable, unless mobilized by TPase
130 supplied *in trans* by an autonomous element (Kunze et al., 1997). *Ac* is a member of the hAT
131 transposon superfamily (named after the founding members *hobo*, *Ac* and *Tam3*; Calvi et al.,
132 1991) and moves via a cut-and-paste mechanism (Bai et al. 2007), with a preference for
133 transposition to linked sites, making the system ideal for local mutagenesis (Greenblatt, 1984;
134 Dooner and Belachew, 1989; Brutnell and Conrad, 2003). To exploit the *Ac/Ds* system for
135 reverse genetics, *Ds* elements have been distributed throughout the genome to provide
136 potential "launch pads" for mutagenesis of nearby genes (Vollbrecht et al. 2010).

137 In this study, we identify five genes encoding components of the CDK8 module in maize,
138 present experimentally determined gene structures, and report expression of corresponding
139 transcripts. We performed *Ds* mutagenesis of the gene *ZmMed12a*, identifying two novel
140 insertional alleles, one of which results in a truncation of the *ZmMed12a* transcript. These
141 insertional mutant alleles will enable determination of the biological roles of the CDK8
142 module in maize development and stress responses.

143

144 **MATERIALS AND METHODS**

145 **Identification of maize CDK8 module genes**

146 Maize CDK8 module genes were identified by BLAST searches using the predicted
147 *Arabidopsis thaliana* protein sequences for HEN3/CDK8 (AT5G63610), CYCC1;1
148 (At5g48640), CCT/MED12 (At4g00450), and GCT/MED13 (At1g55325) available at TAIR
149 (www.arabidopsis.org). Reciprocal BLAST searches were conducted between all maize and
150 *Arabidopsis* sequences, to establish that the five maize genes *ZmCDK8*, *ZmCycC*, *ZmMed12a*,
151 *ZmMed12b*, and *ZmMed13* were the only full length CDK8 homologs present in maize.

152 **Determination of coding sequences for *ZmCDK8*, *ZmCycC*, *ZmMed12a*, *ZmMed12b*, and** 153 ***ZmMed13***

154 Multiple mRNA sequences with full-length coding sequences (as well as upstream and
155 downstream untranslated regions) were identified from the NCBI database for both *ZmCDK8*
156 and *ZmCycC*. For *CDK8*, cDNAs for two alternative splice products were identified:
157 EU968864, NM_001157457 and BT018448 correspond to one splice variant, and BT039744
158 and XR_552425 correspond to the other splice variant. For *CycC*, three independent cDNAs
159 (BT040922, BT033427, and XM008652706) were identified for the one splice variant
160 (shown in Figure 1). Two independent cDNAs (AY105730 and EU972675) represented
161 another *CycC* splice variant with an identical coding sequence but with slight differences in
162 the 3'UTR. A third splice variant was represented by a single cDNA (BT036293); this
163 mRNA has two upstream ORFs, and encodes a truncated *CycC* protein. For *ZmMed12a*,
164 *ZmMed12b* and *ZmMed13*, partial sequences were obtained from the maize database
165 (maizegdb.org), which were then confirmed and extended by RT-PCR using RNA extracted

166 from seedlings of the B73 inbred line. To confirm the *ZmMed12a*, *ZmMed12b*, and
167 *ZmMed13* gene models, we amplified cDNA products covering the entire predicted coding
168 regions. Given their large expected size, *ZmMed12a*, *ZmMed12b*, and *ZmMed13* cDNAs
169 were amplified in multiple over-lapping fragments. Sequencing of cDNA products was
170 generally consistent with gene models based on genomic sequence analysis, except in the
171 case of *ZmMed13*, where a large intron not present in the maize genome sequence was
172 discovered. Coding sequences were deposited in the NCBI database with the following
173 accession numbers: *ZmMed12a* (KP455660), *ZmMed12b* (KP455661), and *ZmMed13*
174 (KP455662).

175 In addition, numerous short genes that are predicted to encode highly truncated ZmMed12
176 proteins of 199 to 431 residues were identified (Núñez-Ríos, 2012). These short *ZmMed12*
177 genes are predicted to encode the Med12 domain (pfam09497) and many have corresponding
178 expressed sequence tags (EST) (B73 RefGen_v3), which do not cover the entire body of
179 these short genes. Analysis of genomic sequences around these predicted coding sequences
180 did not identify additional *Med12* exons (data not shown), suggesting that these are indeed
181 truncated versions of *ZmMed12*, and not mis-annotated genes with nearby exons that would
182 constitute the middle and C-terminal portions of Med12 proteins.

183 **Expression profiles of maize CDK8 module genes**

184
185 Expression data from 22 maize tissues were obtained from <http://qteller.com/qteller3/> on
186 August 2014, in the form of Fragments Per Kilobase of transcript per Million (FPKM). In
187 order to look for correlations between pairs of genes across the tissues, the data was log₂
188 transformed (first adding 1, to avoid the logarithm of 0) and normalized using the
189 normalizeQuantiles function from the limma package (Bolstad et al., 2003).

190
191 The expression values were selected for the 5 CDK8 module genes: *CDK8*
192 (GRMZM2G166771), *CycC* (GRMZM2G408242), *Med12a* (GRMZM2G114459), *Med12b.1*
193 (GRMZM5G828278), *Med12b.2* (GRMZM5G844080), *Med13.1* (GRMZM2G053588), and
194 *Med13.2* (GRMZM2G153792). Since *Med12b.1* and *Med12b.2* as well as *Med13.1* and
195 *Med13.2* are spliced versions of the same gene, the geometric mean was calculated to obtain
196 an averaged estimate of their expression. These data were employed to produce Figure 2A,
197 using the heatmap.2 function from the gplots package (Warns et al., 2015). All pair-wise
198 combinations of the 5 genes across all tissues were plotted using the generic plot function in
199 R (R Core Team, 2015) (Figure S5). The Pearson correlations for all possible pairs of genes
200 were calculated with the cor function, and these data were used as the empirical null to
201 calculate p-values. Correlations for CDK8 module genes were calculated separately. The blob
202 plot in Figure 2B was generated with the corrplot for R.

203

204 **Description of maize stocks**

205 All stocks were maintained in the common genetic background of a color-converted W22
206 inbred line (Dooner & Kermicle, 1971). A stable source of *Ac* transposase was provided by
207 *Ac-immobilized* (*Ac-im*), an *Ac* derivative which has lost 10bp at the 5' end of the element,
208 preventing excision (Conrad and Brutnell, 2005). Activity of *Ac* transposase was monitored
209 using the mutable *Ds* reporter *r1-sc:m3* that carries a *Ds6*-like insertion in the *r1* locus that
210 controls anthocyanin production in the aleurone and scutellum tissues (Alleman and

211 Kermicle, 1993): when *Ac* transposase is present, excision of *Ds* from *r1* restores gene
212 function producing colored sectors (Brutnell & Dellaporta, 1994). The donor *Ds* (*dDs*) stock
213 *dDs-B.S07.0835* was generated by isolation of novel transpositions from *r1-sc:m3* as
214 previously described (Vollbrecht et al., 2010). Presence of *dDs-B.S07.0835* was assayed by
215 PCR as previously described (Vollbrecht et al., 2010) using a combination of the *Ds* end
216 primer JSR05 and a primer specific to the genomic site of B.S07.0835 (5'-
217 GACGCACACACGTCAGTATAG-3'). To generate the test-cross population, plants verified
218 as carrying the donor *dDs-B.S07.0835* with *Ac-im* in the genetic background were used as
219 males to pollinate *r1-sc:m3/r1-sc:m3* female plants.

220 **Seedling screen for transposon insertions in *ZmMed12a***

221 Testcross progeny were germinated and screened for novel insertions of *Ds* in *ZmMed12a*
222 using a PCR-based strategy. Tissue was collected between 7 and 10 days after planting from
223 pools of 10-18 seedlings using a ≈ 3 mm hole punch, and DNA was isolated following a
224 CTAB-based extraction protocol (Weigel and Glazebrook, 2009). A total of 10 *ZmMed12a*
225 gene-specific primers were designed, covering a region extending from 1.8kb upstream of the
226 translational start to the stop codon. These were used in conjunction with the 5' and 3' *Ds*-
227 end primers JSR01 and JGp3, respectively, to amplify DNA adjacent to novel *Ds* insertions
228 in *ZmMed12a* (Table 1). Pools amplifying a product were de-convoluted by screening
229 individuals separately; this second round of PCR used DNA extracted from a different
230 seedling leaf than that sampled for the pool to reduce the chances of recovering somatic
231 transposition events. The PCR products of the second PCR were cleaned (Sambrook and
232 Russell, 2006) and the DNA concentration was adjusted for sequencing by the GENEWIZ
233 Company (South Plainfield, New Jersey, USA). Seedlings carrying putative *med12a*
234 insertional alleles were grown to maturity and propagated by both self-pollination and out-
235 crossing to W22 and B73 inbred lines.

236 **RT-PCR analysis of *zmm12a-1::Ds* and *zmm12a-2::Ds* alleles**

237 DNA was extracted from 10 day old greenhouse grown seedlings of F2 populations
238 segregating the *1::Ds* and *2::Ds* insertions. Seedlings were genotyped using primers to
239 identify homozygous wild type and homozygous insertion alleles for *1::Ds* (primer pair
240 A5.12F and A5.12R for wild type and A5.12F and JGp3 for *Ds* insertion) and *2::Ds* (primer
241 pair C2.7F and C2.7R for wild type allele and C2.7R and JGp3 for *Ds* insertion). RNA was
242 then extracted Trizol (Invitrogen) for wild type and homozygous insertion alleles. Reverse
243 transcription was performed with SuperScript II (Invitrogen). PCR was performed with the
244 following programs, using Kapa Taq Polymerase (Kapa Biosystems). TNC4-TNC5 primer
245 pair: initial denaturation 95 °C 5'; 10 cycles of 95 °C 30'', 60 °C 30'' (-0.5 °C per cycle),
246 72 °C 45''; 27 cycles of 95 °C 30'', 55 °C 30'', 72 °C 45''; final extension 72 °C 5'. RS170-
247 RS167 and ZmCDK primer pairs: initial denaturation 95 °C 5'; 30 cycles of 95 °C 30'',
248 60 °C 30'', 72 °C 1'; 72 °C 10'.

249

250

Table 1: PCR primers used in this study
--

Name	Sequence	Purpose
B.S07.0835	5'-GACGCACACACGTCAGTATAG-3'	Donor Ds site
JGp3	5'-ACCCGACCGGATCGTATCGG-3'	Ds specific
JSR01	5'-GTTTCGAAATCGATCGGGATA-3'	Ds specific
JSR05	5'-CGTCCCGCAAGTTAAATATGA-3'	Ds specific
5'UTRF	5'-TGCACTGCTGCTGTCCTATT-3'	<i>ZmMed12a</i> specific- Ds tagging
E03R	5'-TGGTCCATAACTCAGACATACTTGT-3'	<i>ZmMed12a</i> specific- Ds tagging
E03F	5'-CTCCCTAATACCCCTGTATTTCA-3'	<i>ZmMed12a</i> specific- Ds tagging
E07R	5'-GCATTTGGTAGTAAACAAGAGATGG-3'	<i>ZmMed12a</i> specific- Ds tagging
E06F	5'-CCTTGTTAGAATGCGGTCAA-3'	<i>ZmMed12a</i> specific- Ds tagging
E09.2R	5'-TCAGGACGAACATACTAAGCA-3'	<i>ZmMed12a</i> specific- Ds tagging
INT02F	5'-ACCAAGTTTGTCTCAGGTCAACG-3'	<i>ZmMed12a</i> specific- Ds tagging
E10.2R	5'-CTACCGAAAACCCATGTTGG-3'	<i>ZmMed12a</i> specific- Ds tagging
E10.2F	5'-GCAGCTTTTGAGAGGTTTGAA-3'	<i>ZmMed12a</i> specific- Ds tagging
E12R	5'-GCAACTCCGTCAGCCTTAG-3'	<i>ZmMed12a</i> specific- Ds tagging
RS170	CTGGCGAAAGCCTTTTTGAGAAGC	RT-PCR for Ds insertion
RS167	CCCCACAGGCCCTAACTAAAACA	RT-PCR for Ds insertion
TNC4	CCATATGAGGAACTTCACTCCAG	RT-PCR for Ds insertion
TNC5	ACCTGTACAGAAGTCTGTTAAGCAA	RT-PCR for Ds insertion
ZmCDKF	GGAAGGTATGCACAGGACAGAT	RT-PCR for Ds insertion
ZmCDKR	TTCAGCACAATCTTGCCAAAAC	RT-PCR for Ds insertion

C2.7 F	ACCCAGGAATCCACTCACTTTT	Genotyping F2 for 2:: <i>Ds</i>
C2.7 R	TGCAATCAATAATAGCGTCCAG	Genotyping F2 for 2:: <i>Ds</i>
A5.12 F	AACGTGTAGACCTTGGGTTGAAT	Genotyping F2 for 1:: <i>Ds</i>
A5.12 R	AGGCGTATAGCGGCTAAGGA	Genotyping F2 for 1:: <i>Ds</i>

251

252

253 RESULTS

254 The maize genome encodes all four components of the CDK8 module of Mediator

255 A previous effort to identify Mediator genes from many plant species identified a single
 256 maize homolog for all four CDK8 module genes (*CDK8*, *CYCC*, *MED12* and *MED13*)
 257 (Mathur et al., 2011). In order to conclusively define the number and identity of CDK8
 258 module homologs in maize, we performed BLAST searches to identify all maize gene-
 259 models (B73 reference genome v3; www.maizesequence.org) whose putative protein
 260 products exhibit a high degree of similarity to the entire predicted *Arabidopsis* proteins of the
 261 CDK8 module of Mediator: *CDK8* (encoded by *HEN3*) (Wang and Chen, 2004); *CYCC1*;1
 262 or *CYCC1*;2 (Wang et al., 2004); *MED12* (encoded by *CCT/CRP*) (Gillmor et al., 2010;
 263 Imura et al., 2012); and *MED13* (encoded by *GCT/MAB2*) (Gillmor et al., 2010; Ito et al.,
 264 2011) (Table 2). Using the translated experimentally verified coding sequences for all maize
 265 CDK8 module genes (see below), all potential orthologous relationships were further
 266 validated by reciprocal searching of the *Arabidopsis* genome using maize sequences, and by
 267 inspection of the next-best-hit in both *Arabidopsis*-to-maize and maize-to-*Arabidopsis*
 268 searches (data not shown).

Table 2: Components of Human, Arabidopsis, and Maize CDK8 modules

Human	Hs GenBank mRNA	Arabidopsis	<i>At</i> Model ¹	<i>At</i> GenBank mRNA	Maize	<i>Zm</i> Model ²	<i>Zm</i> GenBank Locus	<i>Zm</i> GenBank mRNAs ⁴
CDK8	P49336	<i>HEN3</i>	AT5G6361 0.1	AAT36644	<i>ZmCDK8</i>	GRMZM2G 166771	LOC100284 562	EU968864, NM_00115745 7, BT018448; BT039744, XR_552425
CYCC	P24863	<i>CYCC1;1</i>	AT5G4864 0.1	BX833973	<i>ZmCYCC</i>	GRMZM2G 408242	LOC100193 909	BT040922, BT033427, XM008652706 ; AY105730, EU972675; BT036293

		<i>CYCC1;2</i>	AT5G4863 0.1 AT5G4863 0.2	AY085977 BT024473	N/A	N/A	N/A	N/A
MED12	NP_00511 1	<i>CCT/CRP</i>	AT4G0045 0.1	AB690341	<i>ZmMed12a</i>	GRMZM2G 114459	LOC103630 556	KP455660
					<i>ZmMed12b</i>	GRMZM5G 828278/ GRMZM5G 844080 ³	LOC100384 108	KP455661
MED13	NM_0051 21	<i>GCT/MAB2</i>	AT1G5532 5.2	N/A	<i>ZmMed13</i>	GRMZM2G 053588/ GRMZM2G 153792 ³	LOC1002799 / LOC1036381 3	KP455662
¹ TAIR gene models [www.arabidopsis.org] ² Maize gene models B73 Reference Genome v3 [maizegdb.org] ³ Split gene annotation ⁴ Independent mRNAs containing full length coding sequences are listed for each splice product. Different splice products are separated by a semi-colon.								

269

270 A single maize gene (GRMZM2G166771) was identified as a potential ortholog of
 271 *HEN3/CDK8*, and designated *ZmCDK8*. Two different full-length splice products were
 272 identified for this gene (EU968864 and BT039744), predicted to encode a full-length and a
 273 truncated maize CDK8 protein (Figure 1A; Figure S1). The full-length *ZmCDK8* protein is
 274 471 amino acids (AA), and shows 73% identity with the 470 AA Arabidopsis CDK8 protein,
 275 and 43% identity with the 464 AA human CDK8 protein (Figure S1). The smaller *ZmCDK8*
 276 protein is 385 AA, primarily because of a truncation of the C terminal domain, and shows
 277 75% identity with Arabidopsis CDK8, and 43% identity with human CDK8. This truncation
 278 occurs after the CDK8 kinase catalytic domain (cd07842), and is thus unlikely to interfere
 279 with the kinase function of the protein (Figure S1).

280 Although Arabidopsis *CYCC* is encoded by a tandem-duplicated gene pair (Wang et al.,
 281 2004), a single potential maize ortholog of *CYCC* (GRMZM2G408242) was identified, and
 282 designated *ZmCycC*. Figure 1B shows the splice product represented by the full-length cDNA
 283 clone BT040922 (Figure 1B). The 257AA BT040922 protein is 42% identical to human
 284 *CycC* and 67% identical to Arabidopsis *CycC1;1* (Figure S2), and contains the Cyclin
 285 domain (cd00043) that is present in human and Arabidopsis *CycC* (Figure S2).

286 BLAST searches using the Arabidopsis *CCT/MED12* protein identified two putative full-
 287 length maize genes (GRMZM2G114459 on chromosome 1, and the split gene
 288 GRMZM5G828278 / GRMZM5G844080 on chromosome 9), which were designated
 289 *ZmMed12a* and *ZmMed12b*. Partial cDNA sequences were publicly available for *ZmMED12a*
 290 and *ZmMed12b*; these sequences, as well as coding sequences predicted by the maize
 291 database, were used to experimentally determine mRNA sequences for both genes by RT-
 292 PCR. The exon-intron structure of both genes is very similar, with the only differences
 293 occurring in the length and position of exons 2, 3 and 4 (Figure 1C&D). These splicing
 294 differences lead to several small insertions or deletions in the N-terminal portions of the
 295 *ZmMed12* proteins, with *ZmMed12a* encoding a protein of 2193AA, and *ZmMed12b*
 296 encoding a protein of 2202AA; the two *ZmMed12* proteins are 91% identical (Figure S3).
 297 *ZmMed12a* is 19% identical to human *Med12*, and 46% identical to Arabidopsis *MED12*;

298 ZmMed12b is 20% identical to human Med12, and 46% identical to Arabidopsis MED12
299 (Figure S3). The region of highest identity is that comprising the Med12 domain
300 (pfam09497), located at the N-terminus of the Med12 proteins (Figure S3).

301 A single maize gene was identified corresponding to *GCT/MED13* (split gene
302 GRMZM2G053588 / GRMZM2G153792), and designated *ZmMed13*. Partial cDNA
303 sequences were publicly available for *ZmMed13*; these sequences were used as the basis for
304 RT-PCR experiments to identify full-length mRNA and coding sequences, which
305 demonstrated that *ZmMed13* encodes a protein of 1892 AA, with 20% identity to human
306 Med13, and 49% identity to Arabidopsis MED13 (Figure 1E & Figure S4).

307 **Maize CDK8 module genes are expressed throughout development**

308 In other organisms where the CDK8 module has been studied, the gene pairs *CDK8* and
309 *CyclinC*; and *Med12* and *Med13*, have similar expression patterns and mutant phenotypes
310 (Yoda et al., 2005; Loncle et al., 2007; Gillmor et al., 2010; Gillmor et al., 2014). In order to
311 determine whether the *CDK8 / CycC* and *Med12 / Med13* genes have similar expression
312 patterns in maize, we used publicly available RNA sequence data to quantify CDK8 module
313 gene expression in different tissues and at different developmental stages (see Materials and
314 Methods). As seen in the heatmap in Figure 2A, *CycC* was expressed at much higher levels
315 in all tissues than the other CDK8 module genes, with *CDK8* and *Med12a* the next highest
316 expressed genes, and *Med13* and *Med12b* with the lowest expression levels

317 In order to more precisely compare tissue-specific expression between the different CDK8
318 module genes, we made pairwise comparisons for all five genes (Figure 2B & Figure S5).
319 Expression was most highly correlated for *Med13* and *Med12b* (Pearson's $r = 0.93$), where
320 the expression ratio between the two genes was close to 1 (compare dotted red line for r , with
321 solid black line representing a 1:1 expression ratio) (Figure 2B & Figure S5). *Med12a* and
322 *Med12b* ($r = 0.77$); *Med12a* and *Med13* ($r = 0.7$); and *CDK8* and *Med12a* ($r = 0.76$) also had
323 high Pearson's coefficients for pairwise comparisons (Figure 2B & Figure S5). By contrast,
324 *CycC* showed almost no correlation with any of the other CDK8 module genes (Figure 2B &
325 Figure S5). The fact that *CycC* shows little expression correlation with the other CDK8
326 module genes, and is expressed at higher levels than *CDK8*, and many times higher than
327 *Med13*, *Med12a* and *Med12b*, suggests that *CycC* may play more varied roles in development
328 and physiology than the other CDK8 module genes.

329 **Maize Med12 is encoded by the duplicated gene pair *ZmMed12a* and *ZmMed12b***

330 The high degree of similarity between *ZmMed12a* and *ZmMed12b* suggests that they are the
331 result of a recent duplication event (Figure S6). *ZmMed12a* and *ZmMed12b* are located in
332 homologous regions of the genome (1S and 9L, respectively), which derive from a
333 polyploidy event that occurred 5-12 million years ago, sometime after the divergence of
334 maize and sorghum lineages. Although gene loss has reduced the number of genes in present-
335 day maize close to pre-duplication levels, in certain cases both syntenic paralogs have been
336 retained (Schnable et al., 2011). Further inspection revealed a sorghum *Med12* gene
337 (Sb01g050260; *SbMed12*) to be present in a region on Chromosome 1L syntenic to the two
338 maize *ZmMed12* containing regions. Moving up- and downstream from *SbMed12*, micro-
339 synteny was conserved, although, typically, for any given sorghum gene only one candidate

340 ortholog was identified in maize, in either the 1S or 9L region, presumably as the result of
 341 gene-loss within paralog pairs following whole genome duplication (Fig. 3).

342

343 **Reverse genetics strategies to target maize CDK8 components**

344 To initiate functional analysis of the maize CDK8 module, we identified publicly available
 345 seed stocks carrying *Ac/Ds* or *Mu* family transposons inserted into, or close to, maize CDK8
 346 module encoding genes (Table 3). On the basis of this search, we selected *ZmMed12a* as our
 347 first target for reverse genetics: at ~56kb, the closest potential *Ds* donor was nearer to
 348 *ZmMed12a* than to any of the other genes. In addition, the availability of a well-characterized
 349 *med12* mutant in *Arabidopsis* provides possibility for comparative study (Gillmor et al.,
 350 2010; Imura et al., 2012; Gillmor et al., 2014). Finally, the retention of two *Med12* syntenic
 351 paralogs in maize suggests that the roles of *ZmMed12a* and *ZmMed12b* are functionally
 352 different, a question which can be addressed by characterization of maize *med12* mutant
 353 alleles.

354

Maize	Maize Accession	Position (kb)	Closest <i>Ac/Ds</i> ¹	Uniform <i>Mu</i> ^{2,3}	<i>Mu</i> Illumina ²
<i>ZmCDK8</i>	GRMZM2G166771	Chr5: 45,538,294- 45,544,117	8311.3 kb	3' UTR	5' UTR
<i>ZmCYCC</i>	GRMZM2G408242	Chr7: 137,095,918- 137,100,956	420 kb	Upstream	5' UTR
<i>ZmMED12a</i>	GRMZM2G114459	Chr1: 2,088,572- 2,102,312	56.2 kb	Upstream (3), 5' UTR (4), Int	
<i>ZmMED12b</i>	GRMZM5G828278 /GRMZM5G844080	Chr9: 155,361,528 155,373,747	717.1 kb	5' UTR (3), Ex	
<i>ZmMED13</i>	GRMZM2G053588 /GRMZM2G153792	Chr9: 28,392,287- 28,413,513	226.7 kb		

¹acdstagging.org; ²*Mutator* resources available at maizeGDB.org; ³Upstream indicates within 1kb 5' of the translational start; numbers in parentheses indicate multiple insertions

355

356

357

358 **Identification of novel *Ds* insertions into *ZmMed12a***

359 To use the *Ac/Ds* transposon system to generate mutant alleles of *ZmMed12a*, we first
 360 obtained donor *Ds* (*dDs*) stocks carrying the *Ds* element *dDs-B.S07.0835*, located 56.2 kb
 361 from *ZmMed12a* (acdstagging.org). The position of the linked *Ds* element was confirmed by
 362 PCR assay (see Materials and Methods) (Conrad and Brutnell, 2005). Presence of *Ac-im* in
 363 testcross progenitor seed stocks was monitored by somatic excision of a second *Ds* from the
 364 *r1-sc:m3* marker locus, resulting in variegated spotting of the kernel aleurone and scutellar
 365 tissues (Figure 4A & B). Spotted kernels were planted and seedlings genotyped for the
 366 presence of *dDs* using a PCR assay (Materials and Methods). To generate novel germinal
 367 insertions into *ZmMed12a*, individuals carrying the *dD* and the *Ac-im* transposase source
 368 were used as males to pollinate T43 (*r-sc:m3/r-sc:m3*) females. A test cross population of 59

369 ears was obtained for the *ZmMed12a* screen (Figure 4A&B).

370 The test-cross population was screened for *Ds* insertions in *ZmMed12a* using combinations of
371 gene specific and *Ds* specific PCR primers (see Materials and Methods). Pools of 10-18
372 seedlings were assayed for amplification of putative *Ds*-flanking junction products (see
373 Figure 4C for example for the *Zmmed12a-2::Ds* insertion). Seedlings constituting the pools
374 from which products were amplified were re-screened separately to identify positive
375 individuals (Figure 4D). This second PCR was performed using DNA extracted from a leaf
376 different from that used for the pool PCR to reduce the rate at which we recovered somatic
377 transposition events. We screened a total of 3,049 seedlings and identified two novel
378 insertions into *ZmMed12a*: *zmmed12a-1::Ds*, located 918bp upstream of the translational
379 start, and *zmmed12a-2::Ds* located in exon 10 (Figure 1C). We performed additional PCR
380 reactions to recover both flanks of the *zmmed12a-1::Ds* and *zmmed12a-2::Ds* insertions.
381 Flanking DNA products were sequenced, confirming the location of the insertions and
382 identifying characteristic 8bp target site duplications. The seedlings carrying the two novel
383 *zmmed12a* insertional alleles were grown to maturity and propagated by both self-pollination
384 and out-crossing. Progeny were germinated and genotyped, confirming the heritability of
385 novel *Ds* insertions (Figure 4E).

386 **The 2::Ds insertion results in a truncated *ZmMed12a* transcript**

387 In order to determine the effect of these novel *Ds* insertions on the *ZmMed12a* gene, we
388 performed RT-PCR analysis of plants homozygous for the wild type and *Ds* alleles, using
389 primer pairs that amplify fragments in exon 9 (downstream of the 1::Ds insertion, and
390 upstream of the 2::Ds insertion), and exon 12 (downstream of both *Ds* insertions) (Figure 4F).
391 Both primer sets amplified fragments from wild type and the *zmmed12a-1::Ds* allele,
392 suggesting that the 1::Ds insertion has no significant effect on the *ZmMed12a* transcript, a
393 result which is not surprising, since this *Ds* insertion is upstream of exon 1. In the case of the
394 *zmmed12a-2::Ds* allele, the primer pair in exon 9 produced an amplification product, while
395 the primer pair in exon 12 showed no amplification from homozygous 2::Ds plants. This result
396 demonstrates that the 2::Ds insertion causes production of a truncated version of the
397 *ZmMed12a* transcript, likely causing a loss of function of the *ZmMed12a* gene.

398

399 **DISCUSSION**

400 In this study we have identified the five genes encoding the CDK8 module of Mediator in
401 maize, determined their coding sequences, characterized their expression in maize tissues
402 during development, and examined the synteny of maize and sorghum in the region of the
403 *Med12* genes. Additionally, we have mutagenized the *ZmMed12a* gene using the *Ac/Ds*
404 transposon system created by Vollbrecht et al. (2010).

405 In our analysis of CDK8 module genes, we identified two alternative transcripts for *CDK8*
406 (Figure 1). One predicted CDK8 protein is significantly shorter than the other, lacking the C-
407 terminal 86 AA. This truncation seems unlikely to affect enzyme activity *per se*, as the
408 kinase domain is intact (Figure S1). However, the lack of this domain may alter regulation of
409 the kinase activity. Alternatively, the truncation may modify the interaction of CDK8 with

410 CycC, or affect the formation of the four protein CDK8 complex. This complex sterically
411 inhibits the interaction of Core Mediator with RNA pol II, by making direct contact with
412 Core Mediator (Tsai et al., 2013). In the case of CycC, one only one isoform was represented
413 by multiple independent cDNAs. Only single splice products were identified for *Med12a*,
414 *Med12b* and *Med13* (Figure 1). One explanation for this is that there is indeed only one splice
415 product for each gene in maize. It is also possible that the very large size of the mRNAs for
416 these three genes (6-7 kb) makes cloning of multiple splice products difficult, due to
417 technical difficulties in cloning such large cDNAs.

418 In our analysis of the relative expression of CDK8 module genes, we found *CDK8* and *CycC*
419 to be more highly expressed in all tissues than *Med12a*, *Med12b* or *Med13*. In particular,
420 *CycC* showed the highest expression in all tissues, consistently 3-4 times higher even than
421 *CDK8* (Figure 2). This increased expression of *CycC* is consistent with roles of CycC
422 beyond regulating transcription in tandem with CDK8 (the best known role for CycC) (Allen
423 and Taatjes, 2015). In addition to regulation of transcription, CycC has been shown to
424 promote the G0 to G1 cell cycle transition through phosphorylation of Retinoblastoma,
425 allowing quiescent cells to enter the cell cycle. CycC achieves this through interaction with
426 CDK3, a kinase that is not associated with transcriptional activation, but instead promotes
427 cell cycle entry (Ren and Rollins, 2004). CycC has also been demonstrated to be a
428 haploinsufficient tumor suppressor in mammals, whose loss of function in mice is lethal
429 during embryogenesis (Li et al., 2014). The haploinsufficiency of CycC may require its
430 mRNA or protein levels to be stably maintained, suggesting an explanation for its high levels
431 in all the tissues that we examined (Figure 2 & Figure S6). *Med12a*, *Med12b*, and *Med13*
432 show much lower expression levels, which also vary considerably between different tissues
433 (Figure 2 & Figure S6). The similar expression profiles for *Med12* and *Med13* in maize are
434 consistent with Arabidopsis, where similar expression profiles for these two genes were
435 reported (Gillmor et al., 2010; Ito et al., 2011; Imura et al., 2012; Gillmor et al., 2014). The
436 widely varying expression levels for *Med12* and *Med13* in different tissues are consistent
437 with various roles for these genes in development, both in primordia (where they show the
438 highest expression), as well as in differentiating and more mature tissue.

439 In Arabidopsis, *MED12* is a single copy gene, with mutant phenotypes in both development
440 and pathogen responses (Gillmor et al., 2010; Imura et al., 2012; Gillmor et al., 2014; Zhu et
441 al., 2014). In maize, however, two *Med12* genes were identified. Sometime after divergence
442 with sorghum, the maize lineage underwent whole genome duplication (Schnable et al.,
443 2011). While in the majority of cases resulting additional gene copies have been lost, for
444 ~10% of the original gene set syntenic paralog pairs have been retained (Hughes et al., 2015).
445 The genomic location of *ZmMed12a* and *ZmMed12b* is consistent with them representing
446 such a paralog pair. In the region of synteny between maize and sorghum, other genes
447 surrounding *Med12* have been reduced to a single copy, suggesting that the retention of both
448 paralogs of *Med12* in maize may have functional significance. Our isolation of the 2::Ds
449 insertional allele of *ZmMed12a* will allow us to test the functional importance of this gene.
450 The truncation of the *ZmMed12a* transcript in the 2::Ds allele makes it very likely that this
451 allele causes a loss of function: a T-DNA insertion in a similar location of the *CCT (MED12)*
452 gene of Arabidopsis causes a strong loss of function phenotype, even when some aberrant
453 transcript is produced (Gillmor et al., 2010; Gillmor et al., 2014)

454 One additional advantage of *Ds* as a mutagen is that novel transpositions occur into linked
455 sites, meaning that the *Ds* insertions in *ZmMed12a* can be remobilized to create further allelic
456 variation in *ZmMed12a*. In addition to mutant alleles that cause a complete loss of function,
457 subsequent *Ds* mutagenesis of *ZmMed12a* may result in hypomorphic alleles that either
458 reduce (but do not eliminate) the function of *ZmMed12a*, or that inactivate specific functional
459 domains of Med12. Alleles that eliminate only certain parts of the Med12 protein could be
460 especially useful in understanding the function of different domains of Med12, currently one
461 of the most interesting, and least explored, aspects of Mediator biology.

462

463 **AUTHOR CONTRIBUTIONS**

464 Study designed by TN-R, KA, TPB, SG and RS. Data acquired and/or analyzed by TN-R,
465 KA, ALA-N, DL-S, CM-C, MG-A, SG, RS. Manuscript written by TN-R, SG and RS, and
466 approved by all authors.

467 **CONFLICT OF INTEREST STATEMENT**

468 The authors declare no conflict of interest.

469 **FUNDING**

470 This study was funded by CINVESTAV institutional funds to CSG and RJHS, CONACyT
471 CB 2009 No. 133990 to MGA, CONACyT CB 2012 No. 151947 to RS, and NSF IOS-
472 0922701 to TPB. CONACyT graduate fellowships supported TN-R, ALA-N (No. 339468),
473 DL-S (No. 262808), and CM-C (No. 20729).

474 **ACKNOWLEDGEMENTS**

475 Thanks to Cei Abreu-Goodger for advice on analysis of gene expression data, and to Jessica
476 Carcaño-Macías for managing seed stocks.

477 **SUPPLEMENTAL MATERIAL**

478 Supplemental Figures S1-S6.

479 **REFERENCES**

480 Alleman, M., and Kermicle, J. L. (1993). Somatic variegation and germinal mutability reflect
481 the position of transposable element Dissociation within the maize R gene. *Genetics* 135,
482 189–203.

483 Allen, B.L. and Taatjes, D.J. (2015). The Mediator complex: a central integrator of
484 transcription. *Nat Rev Mol Cell Biol* 16, 155-166. doi:10.1038/nrm3951

485 Bäckström, S., Elfving, N., Nilsson, R., Wingsle, G., & Björklund, S. (2007). Purification of
486 a plant mediator from *Arabidopsis thaliana* identifies PFT1 as the Med25 subunit. *Molecular*
487 *Cell* 26, 717–729. <http://doi.org/10.1016/j.molcel.2007.05.007>

- 488 Bai, L., Singh, M., Pitt, L., Sweeney, M., and Brutnell, T. P. (2007). Generating novel allelic
489 variation through Activator insertional mutagenesis in maize. *Genetics* 175, 981–992.
490 doi:10.1534/genetics.106.066837.
- 491 Björklund, S., and Gustafsson, C.M. (2005). The yeast Mediator complex and its regulation.
492 *Trends Biochem Sci* 30, 240–244. doi:10.1016/j.tibs.2005.03.008
- 493 Bolduc, N., Yilmaz, A., Mejia-Guerra, M. K., Morohashi, K., O'Connor, D., Grotewold, E.,
494 et al. (2012). Unraveling the KNOTTED1 regulatory network in maize meristems. *Genes Dev*
495 26, 1685–1690. doi:10.1101/gad.193433.112.
- 496 Bolstad, B. M., Irizarry R. A., Astrand, M., and Speed, T. P. (2003). A comparison of
497 normalization methods for high density oligonucleotide array data based on bias and
498 variance. *Bioinformatics* 19, 185–193.
499
- 500 Bourbon, H.-M. (2008). Comparative genomics supports a deep evolutionary origin for the
501 large, four-module transcriptional mediator complex. *Nucleic Acids Research* 36, 3993–4008.
502 doi:10.1093/nar/gkn349
- 503 Brutnell, T. P., and Dellaporta, S. L. (1994). Somatic inactivation and reactivation of Ac
504 associated with changes in cytosine methylation and transposase expression. *Genetics* 138,
505 213–225.
- 506 Brutnell, T.P. and Conrad L.J. (2003). Transposon tagging using Activator (Ac) in maize.
507 *Methods Mol Biol* 236, 157–176. doi:10.1385/1-59259-413-1:157.
- 508 Calvi, B. R., Hong, T. J., Findley, S. D., and Gelbart, W. M. (1991). Evidence for a common
509 evolutionary origin of inverted repeat transposons in Drosophila and plants: hobo, Activator,
510 and Tam3. *Cell* 66, 465–471.
- 511 Candela, H., and Hake, S. (2008). The art and design of genetic screens: maize. *Nat Rev*
512 *Genet* 9, 192–203. doi:10.1038/nrg2291.
- 513 Conrad, L. J., and Brutnell, T. P. (2005). Ac-immobilized, a stable source of Activator
514 transposase that mediates sporophytic and gametophytic excision of Dissociation elements in
515 maize. *Genetics* 171, 1999–2012. doi:10.1534/genetics.105.046623.
- 516 Davidson, R. M., Hansey, C. N., Gowda, M., Childs, K. L., Lin, H., Vaillancourt, B., et al.
517 (2011). Utility of RNA Sequencing for Analysis of Maize Reproductive Transcriptomes. *The*
518 *Plant Genome Journal* 4, 191–13. doi:10.3835/plantgenome2011.05.0015.
- 519 Davis, M. A., Larimore, E. A., Fissel, B. M., Swanger, J., Taatjes, D. J., & Clurman, B. E.
520 (2013). The SCF-Fbw7 ubiquitin ligase degrades MED13 and MED13L and regulates CDK8
521 module association with Mediator. *Genes & Development* 27, 151–156.
522 doi:10.1101/gad.207720.112

- 523 Dooner, H. K., and Kermicle, J. L. (1971). Structure of the R tandem duplication in maize.
524 *Genetics* 67, 427–436.
- 525 Dooner, H.K. and Belachew, A. (1989). Transposition Pattern of the Maize Element Ac from
526 the Bz-M2(ac) Allele. 122, 447–457.
- 527 Elmlund, H., Baraznenok, V., Lindahl, M., Samuelsen, C.O., Koeck, P.J.B., Holmberg, S.,
528 Hebert, H., and Gustafsson, C.M. (2006). The cyclin-dependent kinase 8 module sterically
529 blocks Mediator interactions with RNA polymerase II. *Proc Natl Acad Sci USA* 103, 15788-
530 15793. doi:10.1073/pnas.0607483103
- 531 Flanagan, P. M., Kelleher, R. J., Sayre, M. H., Tschochner, H., & Kornberg, R. D. (1991). A
532 mediator required for activation of RNA polymerase II transcription in vitro. *Nature* 350,
533 436–438. <http://doi.org/10.1038/350436a0>
- 534 Furutani, M., Vernoux, T., Traas, J., Kato, T., Tasaka, M., & Aida, M. (2004). PIN-
535 FORMED1 and PINOID regulate boundary formation and cotyledon development in
536 Arabidopsis embryogenesis. *Development* 131, 5021–5030. doi:10.1242/dev.01388
- 537 Gillmor, C.S., Park, M.-Y., Smith, M.R., Pepitone, R., Kerstetter, R.A., and Poethig, R.S.
538 (2010). The MED12-MED13 module of Mediator regulates the timing of embryo patterning
539 in Arabidopsis. *Development* 137, 113-122. doi:10.1242/dev.043174
- 540 Gillmor, C.S., Silva-Ortega, C.O., Willmann, M.R., Buendía-Monreal, M., and Poethig, R.S.
541 (2014). The Arabidopsis Mediator CDK8 module genes CCT (MED12) and GCT (MED13)
542 are global regulators of developmental phase transitions. *Development* 141, 4580-4589. doi:
543 10.1242/dev.111229
- 544 Greenblatt, I. M. (1984). A chromosome replication pattern deduced from pericarp
545 phenotypes resulting from movements of the transposable element, modulator, in maize.
546 *Genetics* 108, 471–485.
- 547 Imura, Y., Kobayashi, Y., Yamamoto, S., Furutani, M., Tasaka, M., Abe, M., and Araki, T.
548 (2012). *CRYPTIC PRECOCIOUS/MED12* is a novel flowering regulator with multiple target
549 steps in Arabidopsis. *Plant Cell Physiol.* 53, 287-303. doi:10.1093/pcp/pcs002
- 550 Ito, J., Sono, T., Tasaka, M., and Furutani, M. (2011). *MACCHI-BOU 2* is required for early
551 embryo patterning and cotyledon organogenesis in Arabidopsis. *Plant Cell Physiol.* 52, 539-
552 552. doi:10.1093/pcp/pcr013
- 553 Ito, J., Fukaki, H., Onoda, M., Li, L., Li, C., Tasaka, M., Furutani, M., (2016). Auxin-
554 dependent compositional change in Mediator in ARF7- and ARF19-mediated transcription.
555 *Proceedings of the National Academy of Sciences*. doi:10.1073/pnas.1600739113
- 556 Kelleher, R. J., Flanagan, P. M., & Kornberg, R. D. (1990). A novel mediator between
557 activator proteins and the RNA polymerase II transcription apparatus. *Cell*, 61, 1209–1215.

- 558 Knuesel, M. T., Meyer, K. D., Bernecky, C., & Taatjes, D. J. (2009). The human CDK8
559 subcomplex is a molecular switch that controls Mediator coactivator function. *Genes &*
560 *Development*, 23, 439–451. <http://doi.org/10.1101/gad.1767009>
- 561 Kunze, R., H. Saedler, and W.-E. Lonnig. (1997). Plant Transposable Elements. in *Advances*
562 *in Botanical Research*, Academic Press ISBN 978-0-12-005927-0, vol 27, pp350-387.
- 563 Larivière, L., Seizl, M., and Cramer, P. (2012). A structural perspective on Mediator function.
564 *Curr Opin Cell Biol*, 24, 305-313. doi:10.1016/j.ceb.2012.01.007
- 565 Li P., Ponnala L., Gandotra N., Wang L., Si Y., Tausta S. L., Kebrom T. H., Provart N., Patel
566 R., Myers C. R., Reidel E. J., Turgeon R., Liu P., Sun Q., Nelson T. & Brutnell T. P. (2010).
567 The developmental dynamics of the maize leaf transcriptome. *Nature Genetics* 42, 1060–
568 1067. doi:10.1038/ng.703.
- 569 Li, N., Fassel, A., Chick, J., Inuzuka, H., Li, X., Mansour, M. R., et al. (2014). Cyclin C is a
570 haploinsufficient tumour suppressor. *Nat Cell Biol* 16, 1080–1091. doi:10.1038/ncb3046.
- 571 Loncle, N., Boube, M., Joulia, L., Boschiero, C., Werner, M., Cribbs, D. L., & Bourbon, H.-
572 M. (2007). Distinct roles for Mediator Cdk8 module subunits in Drosophila development.
573 *EMBO Journal* 26, 1045–1054. doi:10.1038/sj.emboj.7601566
- 574 Mathur, S., Vyas, S., Kapoor, S., and Tyagi, A.K. (2011). The Mediator complex in plants:
575 structure, phylogeny, and expression profiling of representative genes in a dicot
576 (*Arabidopsis*) and a monocot (rice) during reproduction and abiotic stress. *Plant Physiol.* 157,
577 1609-1627. doi:10.1104/pp.111.18830
- 578 McCarty D. R., and Meeley R. B., (2009). Transposon resources for forward and reverse
579 genetics in maize, in *Handbook of Maize: Genetics and Genomics*, ed. Bennetzen J. L., Hake
580 S., editors. Springer, New York. pp. 561–584
- 581 Ng, S., Giraud, E., Duncan, O., Law, S. R., Wang, Y., Xu, L., et al. (2013). Cyclin-dependent
582 kinase E1 (CDKE1) provides a cellular switch in plants between growth and stress responses.
583 *Journal of Biological Chemistry* 288, 3449–3459. doi:10.1074/jbc.M112.416727
- 584 Plaschka, C., Larivière, L., Wenzek, L., Seizl, M., Hemann, M., Tegunov, D., et al. (2015).
585 Architecture of the RNA polymerase II-Mediator core initiation complex. *Nature* 518, 376-
586 380. doi:10.1038/nature14229
- 587 R Core Team (2015). R: A language and environment for statistical computing. R Foundation
588 for Statistical Computing, Vienna, Austria. URL <https://www.R-project.org/>.
- 589 Ren, S., and Rollins, B. J. (2004). Cyclin C/cdk3 promotes Rb-dependent G0 exit. *Cell* 117,
590 239–251.
- 591 Robinson, P. J., Trnka, M. J., Pellarin, R., Greenberg, C. H., Bushnell, D. A., Davis, R., et al.
592 (2015). Molecular architecture of the yeast Mediator complex. *Elife* 4.
593 doi:10.7554/eLife.08719.
- 594 Sambrook, J., and Russell, D. W. (2006). Purification of PCR products in preparation for

- 595 cloning. *CSH Protoc* 2006, pdb.prot3825. doi:10.1101/pdb.prot3825.
- 596 Schnable, J. C., Springer, N. M., and Freeling, M. (2011). Differentiation of the maize
597 subgenomes by genome dominance and both ancient and ongoing gene loss. *Proceedings of*
598 *the National Academy of Sciences* 108, 4069–4074. doi:10.1073/pnas.1101368108.
- 599 Tsai, K.-L., Sato, S., Tomomori-Sato, C., Conaway, R. C., Conaway, J. W., & Asturias, F. J.
600 (2013). A conserved Mediator-CDK8 kinase module association regulates Mediator-RNA
601 polymerase II interaction. *Nature Structural & Molecular Biology* 20, 611–619.
602 <http://doi.org/10.1038/nsmb.2549>
- 603 Tsai, K.-L., Tomomori-Sato, C., Sato, S., Conaway, R. C., Conaway, J. W., and Asturias, F. J.
604 (2014). Subunit architecture and functional modular rearrangements of the transcriptional
605 mediator complex. *Cell* 157, 1430–1444. doi:10.1016/j.cell.2014.05.015.
- 606 Vollbrecht, E., Duvick, J., Schares, J. P., Ahern, K. R., Deewatthanawong, P., Xu, L., et al.
607 (2010). Genome-wide distribution of transposed Dissociation elements in maize. *Plant Cell*
608 22, 1667–1685. doi:10.1105/tpc.109.073452.
- 609 Wang, W. and Chen, X. (2004). *HUA ENHANCER3* reveals a role for a cyclin-dependent
610 protein kinase in the specification of floral organ identity in Arabidopsis. *Development* 131,
611 3147-3156. doi:10.1242/dev.01187
- 612 Wang, X., Elling, A. A., Li, X., Li, N., Peng, Z., He, G., et al. (2009). Genome-wide and
613 organ-specific landscapes of epigenetic modifications and their relationships to mRNA and
614 small RNA transcriptomes in maize. *Plant Cell* 21, 1053–1069. doi:10.1105/tpc.109.065714.
- 615 Wang, G., Kong, H., Sun, Y., Zhang, X., Zhang, W., Altman, N., DePamphilis, C.W., and
616 Ma, H. (2004). Genome-wide analysis of the cyclin family in Arabidopsis and comparative
617 phylogenetic analysis of plant cyclin-like proteins. *Plant Physiol.* 135, 1084-1099. doi:
618 10.1104/pp.104.040436
- 619 Warnes, G.R., Bolker, B., Bonebakker, L., Gentleman, R., Huber, W., Liaw, A., Lumley, T.,
620 Maechler, M., Magnusson, A., Moeller, S., Schwartz, M., and Venables, B. (2013). gplots:
621 Various R programming tools for plotting data. R package version 2.12.1 available at
622 <http://CRAN.R-project.org/package=gplots>
- 623 Waters, A. J., Makarevitch, I., Eichten, S. R., Swanson-Wagner, R. A., Yeh, C.-T., Xu, W., et
624 al. (2011). Parent-of-origin effects on gene expression and DNA methylation in the maize
625 endosperm. *THE PLANT CELL ONLINE* 23, 4221–4233. doi:10.1105/tpc.111.092668.
- 626 Weigel, D., and Glazebrook, J. (2009). Quick miniprep for plant DNA isolation. *Cold Spring*
627 *Harb Protoc* 2009, pdb.prot5179–pdb.prot5179. doi:10.1101/pdb.prot5179.
- 628 Wu, G., Park, M. Y., Conway, S. R., Wang, J.-W., Weigel, D., & Poethig, R. S. (2009). The
629 sequential action of miR156 and miR172 regulates developmental timing in Arabidopsis. *Cell*
630 138, 750–759. doi:10.1016/j.cell.2009.06.031
- 631 Yin, J.-W. and Wang, G. (2014). The Mediator complex: a master coordinator of
632 transcription and cell lineage development. *Development* 141, 977-987.

633 doi:10.1242/dev.098392

634 Yoda, A., Kouike, H., Okano, H., Sawa, H., (2005). Components of the transcriptional
635 Mediator complex are required for asymmetric cell division in *C. elegans*. *Development* 132,
636 1885–1893. doi:10.1242/dev.01776

637 Zhu, Y., Schluttenhoffer, C. M., Wang, P., Fu, F., Thimmapuram, J., Zhu, J.-K., et al. (2014).
638 CYCLIN-DEPENDENT KINASE8 differentially regulates plant immunity to fungal
639 pathogens through kinase-dependent and -independent functions in *Arabidopsis*. *Plant Cell*
640 26, 4149–4170. doi:10.1105/tpc.114.128611

641

642 FIGURE LEGENDS

643 **Figure 1. The CDK8 module of maize consists of *CDK8*, *CyclinC*, *Med12a*, *Med12b*, and**
644 ***Med13*** (A) Exon-intron structure for two different splice products (EU968864 and
645 BT039744) of the *ZmCDK8* gene (GRMZM2G166771). EU968864 encodes a 471AA protein,
646 while BT039744 encodes a 385AA protein, truncated after the CDK8 kinase catalytic domain
647 (cd07842) (B) Exon-intron structure of mRNA sequence BT040922 for the *ZmCycC* gene
648 (GRMZM2G408242), encoding a predicted protein of 257AA. (C) *ZmMed12a*
649 (GRMZM2G114459) encodes a 2193 AA protein (mRNA sequence KP455660). The
650 location of the *Ds* insertions *Zmmed12a-1::Ds* (918bp upstream of ATG) and *Zmmed12a-*
651 *2::Ds* (exon 10, at bp 4,236 of coding sequence) are indicated. The orientation of each *Ds*
652 insertion is represented by the triangle above the gene (5'-3'), and below (3'-5'). (D)
653 *ZmMed12b* (split gene GRMZM5G828278 / GRMZM5G844080) encodes a 2202 AA
654 predicted protein (mRNA sequence KP455661). (E) *ZmMed13* (split gene
655 GRMZM2G053588 / GRMZM2G153792) encodes a 1892 AA protein (mRNA sequence
656 KP455662). Intron 11 of *ZmMed13* is of unknown size (dotted lines), as it spans a gap in the
657 maize genome sequence. Intron sizes for all genes were determined using corresponding maize
658 genomic sequence. Exons are represented by black boxes, untranslated regions by open boxes,
659 introns by solid black lines, and genomic sequence of *ZmMed12a* upstream of start codon as
660 solid grey line.

661 **Figure 2. CDK8 module genes are broadly expressed in development.** (A) Expression of
662 *Med13*, *Med12a*, *Med12b*, *CDK8* and *CycC* are shown as log₂ (FPKM+1) (Fragments Per
663 Kilobase of exon per Million reads mapped). Data are from the following sources: Mature
664 tassel, Developing ear, Ovule, Seed 5 dap, Seed 10 dap, Embryo 25 dap, Endosperm 25 dap,
665 Silk, Developing tassel, Ear, Seedling leaves field, Seedling leaves gc (growth chamber) from
666 Davidson et al. (2011). Developing leaf and Mature leaf from Li et al. (2010). Seedling roots
667 and Seedling shoots from Wang et al. (2009). Embryo 14 dap and Endosperm 14 dap from
668 Waters et al. (2011). Shoot apex, Ear primordia, Tassel primordia and Leaf primordia from
669 Bolduc et al. (2012). (B) Correlation of expression patterns for pairwise combinations of
670 members of CDK8 module. Positive correlations are shown as blue circles, with larger circles
671 and darker blue signifying greater correlations between the two genes. Gene-by-gene
672 comparisons for all tissue samples are shown in Figure S5, from which r values to make this
673 plot were taken.

674 **Figure 3. Synteny between maize and sorghum genomic regions surrounding *Med12*.**
675 The *Med12* gene is conserved across sorghum and maize syntenic regions. Upper and lower
676 rows: annotated genes in syntenic regions on maize chromosome 1S (*Zm1S*) at ~2Mb (upper
677 row), and maize chromosome 9L (*Zm9L*) at ~155Mb (lower row). Middle row: annotated
678 genes in the region of *SbMed12* at ~73Mb on sorghum chromosome 1L (*Sb1L*). Orthologous
679 genes are connected by dashed lines. *Sb1L* and *Zm9L* run left to right, *Zm1S* runs right to left.
680 Genes are shown as black boxes, and the chromosomes are represented by vertical lines.
681 Regions shown to scale, with the right hand position corresponding to the chromosome
682 location mentioned.

683 **Figure 4. Generation of *Ds* insertional alleles of *ZmMed12a*, and their effect on the**
684 ***ZmMed12a* transcript.** (A) Crossing scheme for generating plants homozygous for the *r-*
685 *sc:m3* reporter allele, and heterozygous for *Ac-immobilized* (*Ac-im*) and the *Ds* insertion
686 linked to *ZmMed12a*. (B) The presence of *r-sc:m3* allows for selection of spotted F1
687 kernels, indicating the presence of *Ac-im*, required for remobilizing the *Ds* insertion
688 linked to *ZmMed12a*. (C) Initial pools of 10-18 seedlings were screened by PCR for the
689 presence of a *Ds* element in *ZmMed12a*, using gene specific primer E10.2 and *Ds* specific
690 primer JGp3. A 1.8 kb fragment (yellow arrow) was amplified from pool C2. (D)
691 Individual plants from pool C2 were tested for the presence of the same fragment, which
692 was amplified from plant 7, denominated C2.7 (*Zmmed12a-2::Ds*) (E) This 1.8kb band
693 segregated in nine progeny of the selfed plant C2.7, demonstrating that it is a heritable
694 germinal insertion. (F) RT-PCR analysis of the effect of the *1::Ds* and *2::Ds* insertions
695 on the *ZmMed12a* transcript. The *1::Ds* insertion has no detectable effect on the stability
696 of the *ZmMed12a* transcript, while the *2::Ds* insertion creates a transcript that is truncated
697 after the *Ds* insertion. The location of the primer pairs used to amplify the transcript are
698 indicated in the gene diagram. *ZmCDK* (GRMZM2G149286) was used as a control gene.
699 One representative experiment of three biological replicates is shown.

Figure 1.TIF

bioRxiv preprint doi: <https://doi.org/10.1101/097204>; this version posted December 28, 2016. The copyright holder for this preprint (which was not certified by peer review) is the author/funder. All rights reserved. No reuse allowed without permission.

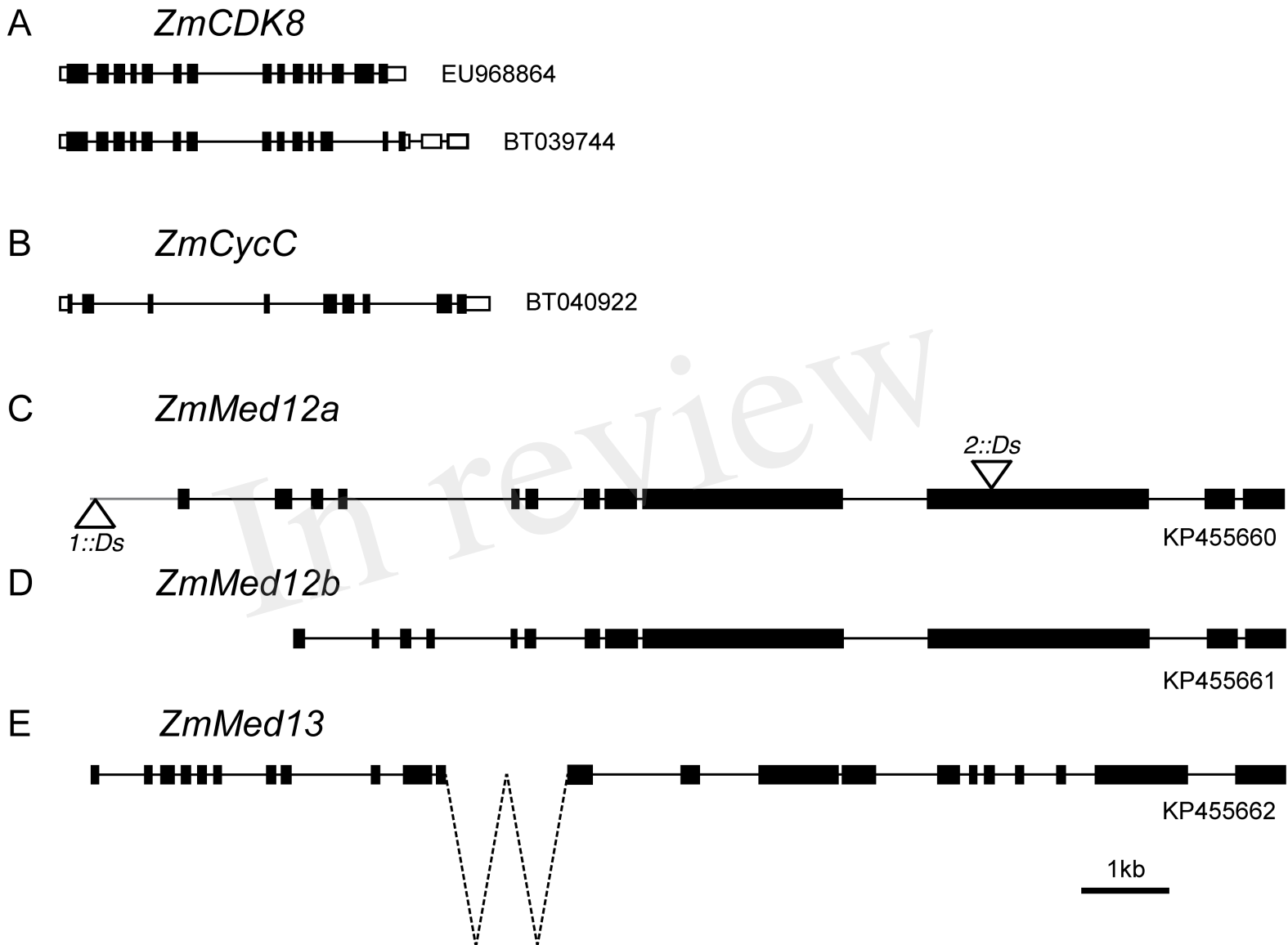


Figure 1

Figure 2.TIF

bioRxiv preprint doi: <https://doi.org/10.1101/097204>; this version posted December 28, 2016. The copyright holder for this preprint (which was not certified by peer review) is the author/funder. All rights reserved. No reuse allowed without permission.

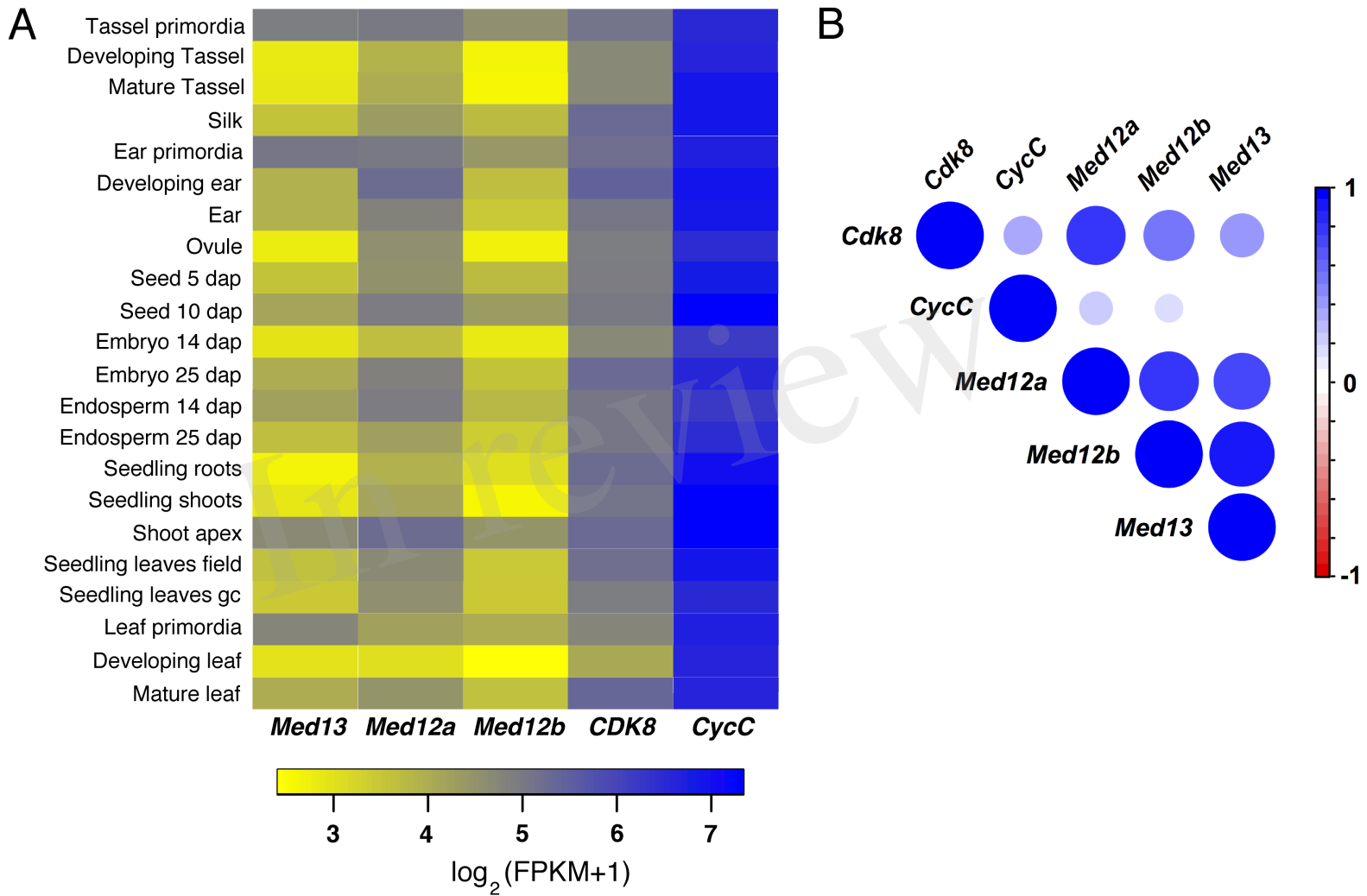


Figure 2

Figure 3.TIF

bioRxiv preprint doi: <https://doi.org/10.1101/097204>; this version posted December 28, 2016. The copyright holder for this preprint (which was not certified by peer review) is the author/funder. All rights reserved. No reuse allowed without permission.

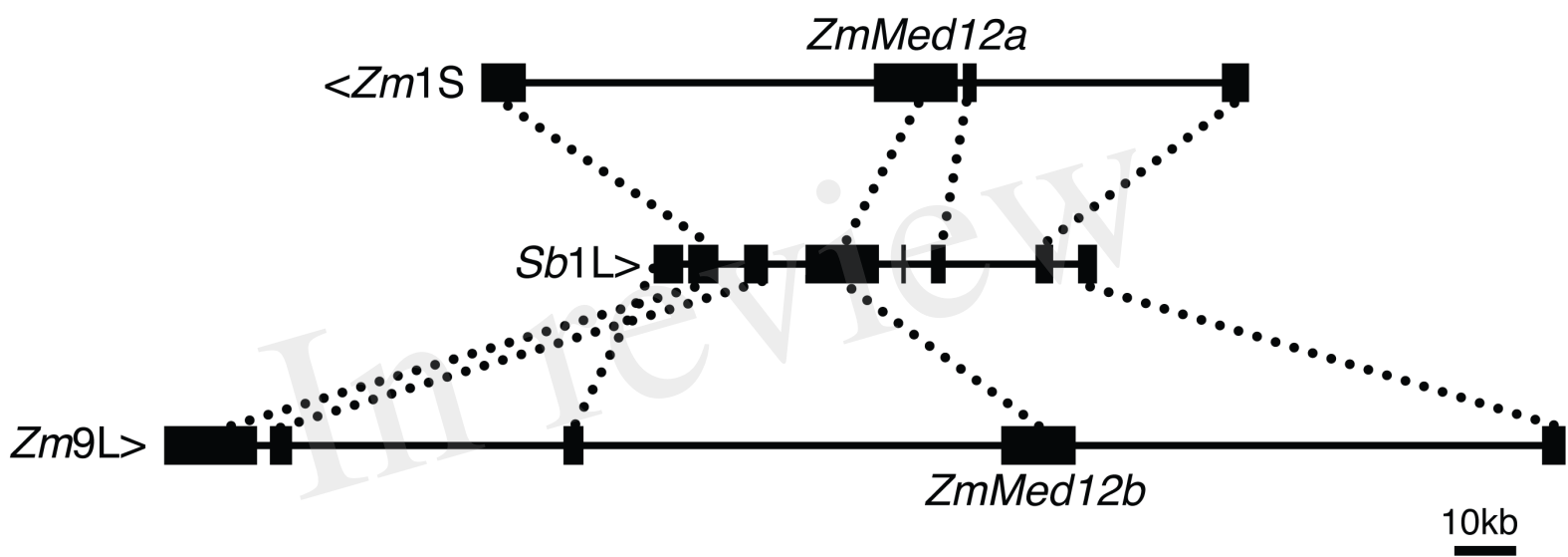


Figure 3

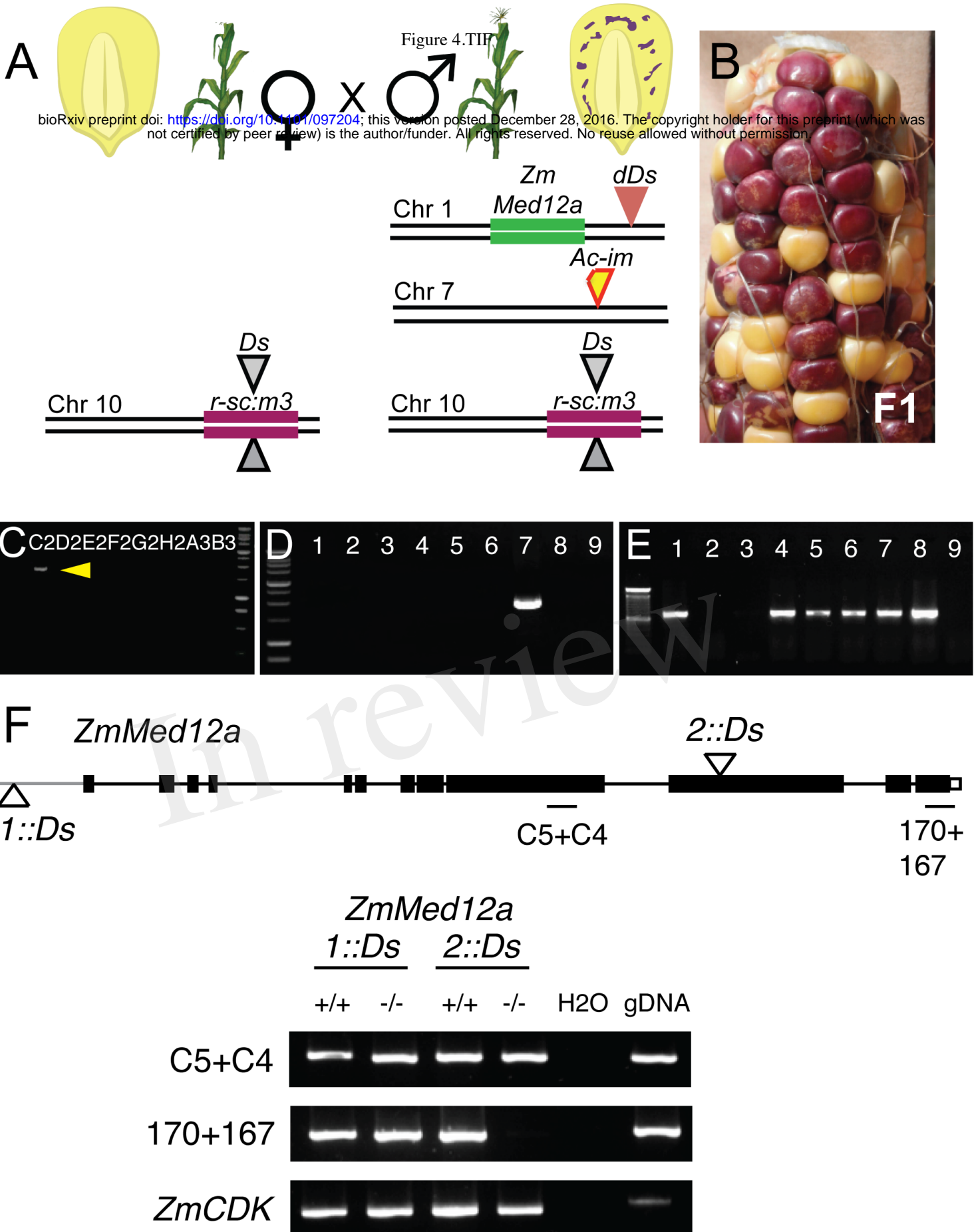


Figure 4